Journal of Theoretical and Applied Information Technology
31st July 2020. Vol.98. No 14

ISSN: 1992-8645 www.jatit.org E-ISSN: 1817-3195

INNOVATION AND INTELLIGENT SYSTEMS IN MODELING AND OPTIMIZING FUSED DEPOSITION MODELING PROCESS PARAMETERS FOR DIMENSIONAL ACCURACY USING SURFACE RESPONSE METHODOLOGY

[1]H. ISKSIOUI*,[1]S. ENNIMA, [1]A. ELGHARAD,[2]M. OUBREK, [3]S. BOUREKKADI

[1]M2SM, Research Center STIS, Dep. of Mechanical Engineering,

ENSET, Mohammed V University, Rabat, Morocco

[2]PCMT, Research Center STIS, Dep. of mechanical engineering,

ENSET, Mohammed V University, Rabat, Morocco

[3]National Engineering School for Mechanics and Aerotechnics (ENSMA), University of Poitiers France.

L2IISR, ARSED Ibn Tofail University, Kenitra Morocco

E-mail: [1]hamza.isksioui@um5s.net.ma

ABSTRACT

Fused Deposition Modeling (FDM) is a 3D printing process (additive manufacturing) that is widely used around the world in a variety of industrial applications due to its ability to create complex 3D parts and geometries. The accuracy of parts printed by FDM technology is greatly influenced by various process parameters which are often difficult to determine. Increasing dimensional accuracy is the major concern of most industrial applications and affects the cost and functionality of the fabricated part. One of the key issues of the FDM process is how to select the right parameter to reduce the dimensional errors.This study offers an optimality criterion to optimize FDM parameters in order to go over the limits of the traditional designs previously used. The influence of the FDM parameters is studied using the D-optimal surface response methodology. Their effects on dimensional accuracy are studied critically. Mathematical model has been formulated to develop a functional non-linear relationship between process parameters and dimensional accuracy. Ultimately, the optimal setting of the process parameters has been determined and the results show that the optimality criterion is a very promising technique to optimize the FDM process parameters.

Keywords: *Additive Manufacturing; Fused Deposition Modeling; Parameters Optimization; Response Surface Method; Dimensional Accuracy*

1. INTRODUCTION

Additive An The Additive Manufacturing Process (AM) creates three-dimensional (3D) parts by sequentially fabricating the material layers [1] without the use of shaping tools. So additive manufacturing (AM) reduces material wastage, is more economical and allows flexibility in geometric complexity unlike traditional subtractive manufacturing processes [2]. In recent years, the manufacturing of parts by additive manufacturing process has increased enormously [3]; so is called Rapid Manufacturing [4, 5]. Additive manufacturing applications focus on products in various fields such as medicine, mechanical engineering, art, fashion [6, 7] and aerospace, which is the second largest market for which AM technology is profitable because of its customization, low volume and high value-added production lines [8, 9].

The AM process is applied to treat different kinds of materials: for example polymers, ceramics and metals, as long as different types of machines are operated. As for polymeric AM polymerization, three main types of additive manufacturing processes are currently available [10]: stereolithography (SLA) [11, 12] based on the use

Journal of Theoretical and Applied Information Technology
31st July 2020. Vol.98. No 14

ISSN: 1992-8645 www.jatit.org E-ISSN: 1817-3195

of photopolymers that can be selectively cured using various sources of energy (the most common being UV). Selective Laser Sintering [13-15], where polymer powders ise used as a base material assembled by laser and Fusion Deposition Modeling (FDM) [16-18], in which the parts are printed from polymeric filaments.

FDM technology is the most popular method, developed by Stratasys. Part of the additive manufacturing technologies allows a fast and clean manufacturing of functional components and prototypes. In this technology, the layers are made by extruding a thermoplastic filament, which is unwound from a coil and sent to the head of the liquefier to produce a part. The semi-molten filament acts to pass through small nozzles of diameter (0.4mm, 0.6mm, 0.8mm, 1.00mm and 1.20mm) where it is melted and then deposited in the form of a thin layer on a heated table as shown in Figure 1 . Once on the bed, the polymer hardens because of cooling. Subsequently, the platform goes down, and the printer proceeds in the same way for the next layers.

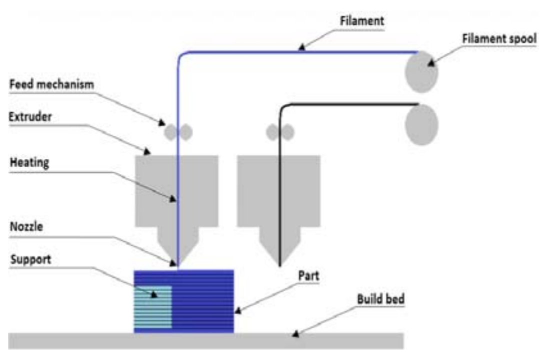

Figure 1: FDM manufacturing process

The filament generally has a circular section with specific diameters for each FDM system. The most used diameters are either 3.0 mm or 1.75 mm. Additive manufacturing processes, including FDM technology, are needed to produce high quality parts. The need of FDM increases in all areas: such as telecommunications, recreation, naval industry, military, medical implants, aerospace and electronics that require an ever-higher level of dimensional accuracy. Some applications require dimensional accuracy with tight tolerances will ensure dimensional repeatability and stability of the printed parts. The dimensional accuracy of the FDM printed part depends greatly on the selected process parameters. FDM-printed parts suffer from dimensional inaccuracy compared to other AM technologies such as SLA or SLS due to the diversity of conflicting process parameters that affect dimensional accuracy individually or collectively in several parameters interactions [19].

This document is composed of: Section 2 the current state of art. Section 3 presents the research methodology used and useful information on the use of optimal designs, including the D-optimality criterion. Section 4 presents an analysis of the data obtained from the experience and mathematical models developed. Section 5 discusses the results. Section 6 presents the conclusions.

2. LITERATURE REVIEW

Some research work has been done to optimize dimensional precision of parts completed in FDM.

Ala aldin Alafaghani [29] studied the influence of FDM processing parameters on the quality of parts and their functionality. The study investigates the effect of parameters independently from mechanical properties and dimensional accuracy.From a Taguchi plan, they have established 18 test samples which were printed using various processing parameters. In order to study the repeatability and resulting tolerances, the dimensions of these specimens were measured and compared to a 3D CAD model. In addition, the study presents a new approach developed for modeling FDM parts using FEA. Nancharaiah et al. [30] applied an experimental method on dimensional accuracy and surface quality using the ANOVA technique and the Taguchi method. However, in this experimental, optimal parameters have not been addressed.Sahu et al. [31] applied the Taguchi Experience Plan to study the effect of process parameters on the accuracy of parts. However, the use of the Fuzzy Inference System (FIS) requires the development of rules. Therefore, it requires a thorough the expertise and prior experience. Tobias Lienekea [32] studied missing restrictions which appear in the available geometric accuracy. The objective of this study was the experimental determination of dimensional tolerances using standard parameters. To that end, a methodical procedure has been put in place. On the basis of the experimentally determined deviations, dimensional tolerances were calculated. Sood et al. [33] experimented the influence of manufacturing parameters on dimensional accuracy using the Experiment Plan Method (Taguchi Plan) and Artificial Neural Networks (ANN). They noted that the optimal manufacturing parameters are different for each quality criterion, indicating that the optimal manufacturing parameters are not obtained. For this reason, the Gray Relational Grade (GRG) was used to turn three responses into one answer. The limitation of this work is that the optimal settings

Journal of Theoretical and Applied Information Technology
31st July 2020. Vol.98. No 14

ISSN: 1992-8645 www.jatit.org E-ISSN: 1817-3195

are limited to experimental values, where, in fact, the optimal settings are not exactly the same as the parameter values used in the experimental matrix. Vijay.B.Nidagundi [34] have studied optimization of process parameters for melt deposition modeling (FDM). Layer thickness, orientation angle, and fill angle are the process variables considered for optimization. Tensile strength, surface roughness, dimensional accuracy and manufacturing time were considered response parameters. The experiments were designed using Taguchi's well-known L9 Orthogonal Network. Taguchi's S / N ratio was used to identify the optimal values of the parameters. The effectiveness of each parameter was studied using an analysis of variance. In the end, the performance of the optimal conditions was validated by a verification experiment. Zhang and Peng [35] studied the relationship between dimensional errors, manufacturing parameters and deformations. They noticed that the optimal manufacturing parameters for deformation and dimensional error vary. However, if the goal is to minimize deformation and dimensional error at the same time, the study could not provide a definitive answer in terms of a global solution to this problem.

The current state of art indicates that during the production, the dimensional accuracy of manufactured parts is influenced by various parameters of the FDM process. Although large optimization studies to reduce the dimensional errors of parts was proposed, they still have some drawbacks and weaknesses. First of all, the majority of previous research work has mainly studied the dimensional accuracy of parts manufactured by ABS and not by PLA (Polylactic Acid). Secondly, traditional experimental designs such as GRG and Taguchi have been used previously to improve the quality of parts. However, traditional processes are too complex to establish a functional relationship between dimensional accuracy and process parameters. Then, there are many studies that use the Taguchi method combined with a global ANN or fuzzy assessment. Indeed, ANN and FIS do not provide sufficient studies on factors and their interaction effects on dimensional accuracy if additional analyzes. However, this approach has its drawbacks, because it takes into account the complexity of the computation process, it requires a large amount of data for appropriate technical judgment to interpret the responses or results. Finally, no study considers all parameters with all possible levels that may be affecting dimensional accuracy. And this is very important to achieve a much improved accuracy and a functional relationship between dimensional accuracy and manufacturing parameters.

Our research work unlike the work of previous studies, attempts to overcome the limitations of previous work by developing a method that can improve dimensional accuracy effectively. This article presents a methodology based on computer-generated optimal designs using a reliable and efficient criterion D optimality to deal with the optimization problem involving many FDM parameters and levels of constraints (irregular experimental matrix) . The proposed methodology has a better performance and accuracy than previous methodologies in several cases. In this work, we have established global relationships between developed the mathematical models and the dimensional accuracy and parameters of the part by PLA (Polylactic Acid). In this study, a complete analysis was provided taking into account all critical process parameters with the possible levels. This proposed and developed method was then validated in terms of accuracy and precision.

3. METHODS AND MATERIALS

3.1 Experimental Work:

In this work, the specimen used has a length of 35 mm, a width of 12.5 mm and a height of 3.5mm. This was designated from the basis of ASTM D5418-07 [20] and references from the TA instrument manufacturer [21] that was presented in Figure 2. A total of 50 samples (shown in Figure 3) that were printed by the 3DP WORKBENCH machine (shown in Figure 4) from 3DP Platform Industries, using a nozzle diameter of 0.6 mm diameter and 1.75 mm diameter filaments and PLA material (Polylactic Acid).

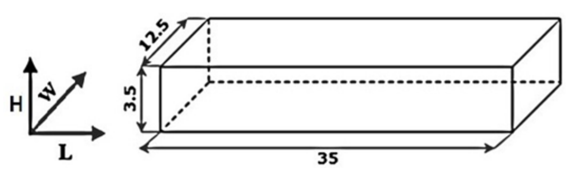

Figure 2: Sample dimensions

Figure 3: printed samples

Journal of Theoretical and Applied Information Technology
31st July 2020. Vol.98. No 14

ISSN: 1992-8645 www.jatit.org E-ISSN: 1817-3195

This FDM printer has a print size of 1000 x 1000 x 500 mm with a resolution of 0.07 mm. Samples were manufactured in the XYZ orientation at the center of construction bed [22]. All models were created in the SolidWorks design and modeling software and converted to standard STL file, the STL file was prepared in the Simplify3d software to generate the toolpath and set all process parameters on all samples. All samples were made using PLA (Polylactic Acid) filaments 1.75 mm in diameter and nozzle diameter 0.6 mm.

The measurements of dimensional accuracy were made using a 3-dimensional CMM-type gantry and CNC-guided measuring machine; they allow high precision measurements of 0.0001 mm and with an optional PH9 probe head. From a point cloud taken from an actual surface (or curve), the machine software proceeds to identify the sensed element.

Figure 4: 3DP workbench used

This operation consists of associating a theoretical surface (or curve) to the cloud of palpated points. The most used association criteria are the Chebyshev criterion or the least squares criterion. MMT has been programmed to perform measurements automatically to avoid errors that may occur during the measurement process during a manual measurement. So, to carry out this program we developed a range of measurement according to:

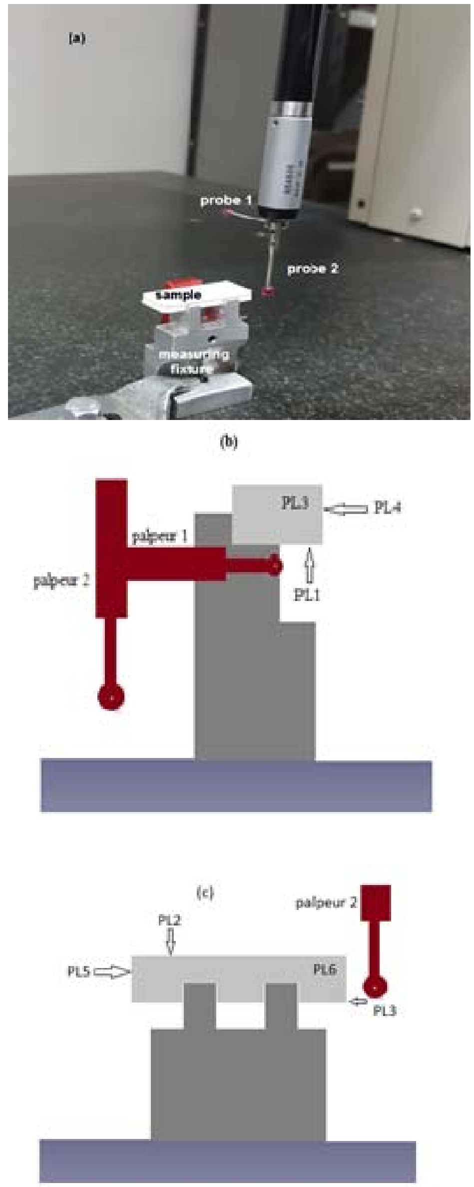

Figure 5: Assembly and fixing of samples (a), Assembly of the probe 1 and probe 2 (b, c).

• The NC program parameters are: Travel speed: 100 mm / s, Measurement speed: 1 mm / s, Safety distance: 1 mm and Maximum length in measuring speed: 2 mm.

• For the positioning of the samples in the MMT table, a mounting device and fixtures were used to fix the samples and to allow repeatability and ease of measurement as shown in Figure 5a.

• Assembly of the probe 1 and probe 2, then calibration of the two probes in diameter and position by measuring the reference sphere. The probe 1 is chosen long enough to reach any plane point PL1, its orientation is substantially parallel to PL1 (see Figure 5b). The probe 2 is chosen long enough to reach any point of the planes PL2, PL3, PL4, PL5 and PL6. Its orientation is substantially perpendicular to the plane PL2 and parallel to the PL3, PL4, PL5 and PL6 planes (see Figure 5c).

- ✓ 5 point probing of the known plane surface PL1.
- ✓ 9 point probing of the known plane surface PL2.
- ✓ 3 point probing of the known plane surface PL3.
- ✓ 4 point probing of the known plane surface PL4.
- ✓ 3 point probing of the known plane surface PL5.
- ✓ 4 point probing of the known plane surface PL6.

From the measurement results of length, width and thickness were made per sample, the following equation 1 was developed to calculate the dimensional error:

$$\Delta D = D_{CAD} - D_{EXP} \quad (1)$$

ΔD Represents the dimensional error, D_{CAD} represents the value of the CAO model and D_{EXP} represents the experimental value.

3.2 Experimental Design:

3.2.1 The designated process elements and their levels:

The quality of an FDM printed model depends primarily on the designated process elements. In this research study the manufacturing parameters that have been treated are defined as follows [23, 24]: Platform temperature (A); Extruder temperature (B); Layer thickness (C); Number of shells (D); Infill density (E); Print speed (F); Infill pattern (G); Number of solid layers 'U / L' (H). Each of the parameters analyzed was assigned to three levels of control as Table 1 presented. The levels of these control parameters are selected from the literature review, their relevance, significance, and experience gained from the preliminary pilot surveys, as well as the maximum and minimum allowed values. Other research work focuses on a single parameter, such as the direction of the building [25], while others focus on 3 or 4 to 6 treatment parameters at the same time. Effects as in [26-28]: where the effect of layer height, the construction direction, the number of shells and other parameters are studied at the same time.

Table 1: Parameters and levels of varying Processing Parameters

Symbols	Factors	Units	Levels
A	Platform temperature	◦C	70 75 80
B	Extruder temperature	◦C	190 200 210
C	Layer thickness	mm	0.15 0.3 0.45
D	Number of shells	–	1 2 3
E	Infill density	%	25 50 75
F	Print speed	mm/s	50 65 80
G	Infill pattern ’H=1 D=2 L=3’	–	H D L
H	Number of solid layers ’U/L’	–	2 3 4

The manufacturing parameters are represented graphically (shown in Fig.6 (a-d)) are defined as follows:

- ✓ (A) Platform temperature is the bed temperature.
- ✓ (B) Extruder temperature is the necessary temperature to melt the material
- ✓ (C) Layer thickness is the thickness of the extruded layer. It is based on the filament and the nozzle diameters (figure5-a).
- ✓ (D) Number of shells is the number of outlines built around the outer and inner pattern. (figure 5-b).
- ✓ (E) Infill density: is the percentage of the infill of the printed part.
- ✓ (F) Print speed: is the printing velocity in mm/s.
- ✓ (G) Infill pattern: is the internal structure of the print H: Honeycomb; D: Grid; L: Rectilinear (figure 5-c).
- ✓ (H) Number of solid layers 'U / L': the number of upper and lower layers (figure 5-d)

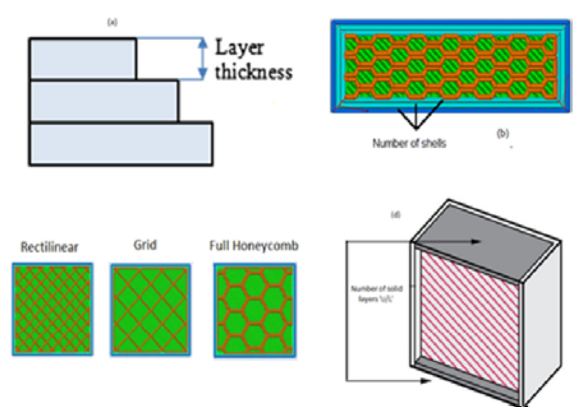

Figure 6: Input parameters, (a) Layer thickness,(b) Number of shells, (c) Infill pattern, (d) Number of solid layers 'U / L'

3.2.2 Developing the experimental design matrix:

The study of eight parameters using traditional experimental designs such as complete factorial requires 256 examinations and Taguchi plan

ISSN: 1992-8645 www.jatit.org E-ISSN: 1817-3195

requires 18 analyses. It should be noted that these numbers of analyses from the complete factorial design are only at two levels of each parameter (standard designs) and the number of analyses from Taguchi plan is not required for processing of complex problems. In addition, Taguchi matrices are not suitable for nonlinear and complex problems because of the higher order of empirical polynomial models that cannot be mapped using these methods, which is very important when that the goal is optimization. Therefore, the D-optimal design proposed in this study offers a better alternative approach, since it provides a better accuracy with only 50 analyses at eight parameters and three levels at each parameter (irregular experimental matrix). The efficiency and accuracy of an experimental model depend on the precise measurement of responses, as well as the detailed planning of experimental procedures. The optimal design improves the accuracy of the models developed by testing the lack of fit and reducing the influence of the design points on the fit regression response. This provided the appropriate degrees of freedom needed and provided an accurate estimate of the variation in responses to develop an adequate relationship between parameters and output responses. Table 2 represents the final design matrix.

4. ANALYSIS

From the D-optimal design matrix, dimensional errors in length, width and thickness were analysed to obtain the results of the different variables responses and to study the effects of the parameters involved. Table 2 presents the experimental results for the three responses of length ΔL, width ΔW and thickness ΔT in each set of operating conditions, based on the D-optimal design. The responses were then analysed to develop the most appropriate mathematical models. For the regression and graphical analysis of the data collected during the experiment, we used MATLAB software. In this study, linear models, interactions, pure quadratic and quadratic were analysed in order to determine the best model in terms of adaptability to experimental data. Table 3 presents the statistical summary of the models.

This table clearly shows that the quadratic model has p-value for the F-test on the weaker model (meaning) and Square root of the mean squared error, which estimates the standard deviation of the error distribution is lower by a for the other modules. In addition, the quadratic model has the highest R-squared and Adjusted R-squared. Moreover, adjusted R-square is in very good agreement. Thus, the quadratic model provides an excellent explanation of the relationship between dimensional accuracy and FDM parameters. It was therefore used in this study.

4.1 Development Of Mathematical Models:

RSM (Response Surface Methodology) is a set of mathematical and statistical techniques useful for improving, developing and optimizing process variables. This is dedicated to the evaluation of the relationships between the controlled experimental factors and the observed results of one or more selected criteria. The RSM consists of a group of techniques used in the empirical study of the relationship between several input variables and a response. If all the variables are supposed to be measurable, the response surface can be expressed as in the function: Y=f (X1;X2;……;Xk). The goal is to optimize the response variable y. The Eq.2 expressed the quadratic regression model used in this study as follows:

$$Y = \beta_0 + \sum_{i=1}^{k} \beta_i X_i + \sum_{i=1}^{k} \beta_{ii} X_i^2 + \sum_{i<j}^{k} \beta_{ij} X_i X_j + \varepsilon \quad (2)$$

- ✓ Y is the predicted response
- ✓ k is the number of variable
- ✓ Xi and Xj are the coded variables
- ✓ β_0 is the constant of the regression equation
- ✓ β_{ii} is the interactive coefficient
- ✓ β_{ij} is the square term of each variable
- ✓ ε is the random measurement error

In matrix form:

$$Y = \beta X + \varepsilon \quad (3)$$

The solution of equation 2 can be obtained by the matrix approach:

$$\beta = (X^T X)^{-1} X^T Y \quad (4)$$

In addition, for the eight parameters, the quadratic model could be formulated in equation 5:

$$\begin{aligned} Y &= \beta_0 + \beta_1 A + \beta_2 B + \beta_3 C + \beta_4 D + \beta_5 E + \beta_6 F + \beta_7 G + \\ &\beta_8 H + \beta_{12} AB + \beta_{13} AC + \beta_{14} AD + \beta_{15} AE + \beta_{16} AF + \\ &\beta_{17} AG + \beta_{18} AH + \beta_{23} BC + \beta_{24} BD + \beta_{25} BE + \beta_{26} BF + \\ &\beta_{27} BG + \beta_{28} BH + \beta_{34} CD + \beta_{35} CE + \beta_{36} CF + \beta_{37} CG + \\ &\beta_{38} CH + \beta_{45} DE + \beta_{46} DF + \beta_{47} DG + \beta_{48} DH + \beta_{56} EF + \\ &\beta_{57} EG + \beta_{58} EH + \beta_{67} FG + \beta_{68} FH + \beta_{78} GH + \beta_{11} A^2 + \\ &\beta_{22} B^2 + \beta_{33} C^2 + \beta_{44} D^2 + \beta_{55} E^2 + \beta_{66} F^2 + \beta_{77} G^2 + \beta_{88} H \end{aligned}$$

(5)

After determining the coefficients, the mathematical models were developed. These models can be used to evaluate and study the relationship between input parameters and the dimensional accuracy required in terms of length, width, and thickness variation by giving levels of each factor, with factor levels specified in the original units. The final models developed, in terms of their actual values for length ΔL, width ΔW and thickness ΔT, are given by equations 6, 7 and 8, respectively:

$$\Delta L = -9.2368 + 0.212A + 0.0035799B - 0.89266C + 0.15864D + 0.017735E + 0.013385F + 0.56082G - 0.091621H - 0.018841AC - 8.5158*10^{-5}AF + 0.0019693AH + 0.008502BC - 7.5847*10^{-5}BE - 0.0019589BG - 0.00058834BH - 0.0022484CE - 0.040393CG - 0.072752CH - 0.0008086DF - 0.0064656DG - 3.792*10^{-5}EF + 0.00035869EH - 0.00047387FG - 0.00089654FH + 0.0087295GH - 0.001351A^2 + 1.5487C^2 - 0.014104D^2 - 0.033656G^2 + 0.018499H^2 \quad (6)$$

Table 2: D-Optimal Design Matrix And Collected Data

RUN	Factors								Responses	
	A	B	C	D	E	F	G	H	T	M
1	80	210	0.45	3	25	80	L	4	3	2.27
2	80	210	0.45	1	75	50	L	4	4	2.28
3	70	190	0.15	3	75	65	H	4	7	1.78
4	70	210	0.15	1	75	50	H	3	8	1.66
5	80	190	0.15	3	25	80	H	4	5	1.5
6	80	210	0.45	1	75	80	H	2	2	1.99
7	80	190	0.45	3	75	50	D	4	3	2.27
8	80	190	0.15	1	75	80	H	2	5	1.61
9	70	210	0.15	3	25	50	L	4	8	1.52
10	70	210	0.45	3	25	80	H	4	3	2.27
11	70	200	0.45	1	25	50	D	4	4	2.28
12	80	190	0.45	1	25	50	L	4	4	2.28
13	70	210	0.15	1	75	80	L	2	5	1.74
14	80	190	0.45	1	75	80	L	2	2	2.08
15	80	190	0.45	1	75	50	H	2	3	1.99
16	70	190	0.15	1	25	65	L	2	4	1.08
17	70	190	0.45	2	25	50	H	3	3	2.02
18	70	190	0.45	3	50	80	L	4	3	2.27
19	70	190	0.15	3	75	50	L	2	8	1.83
20	80	190	0.45	1	75	80	H	4	3	2.28
21	80	190	0.3	3	25	50	L	2	4	1.64
22	80	210	0.15	1	25	50	L	2	5	1.08
23	80	190	0.15	1	50	50	H	4	7	1.48
24	80	210	0.15	1	50	80	L	4	5	1.55
25	70	210	0.45	2	75	80	D	4	3	2.28
26	70	210	0.45	1	25	80	L	3	2	1.97
27	70	210	0.45	1	25	50	H	2	3	1.65
28	70	200	0.15	1	25	80	H	4	4	1.28
29	70	200	0.15	3	75	80	L	3	6	1.86
30	80	210	0.15	3	25	80	L	2	5	1.38
31	70	190	0.45	3	25	80	L	2	2	1.84
32	70	210	0.3	3	75	65	D	2	4	2.1
33	75	190	0.15	2	25	80	L	4	5	1.42
34	70	190	0.45	1	75	80	H	2	2	1.99
35	70	200	0.45	2	50	50	L	2	3	1.93
36	80	210	0.15	3	75	50	H	2	8	1.71

37	80	200	0.15	2	75	65	L	4	7	1.85
38	80	210	0.45	3	25	50	D	2	3	1.89
39	70	210	0.45	3	75	50	H	4	3	2.27
40	75	210	0.45	1	50	65	H	4	3	2.28
41	75	200	0.15	3	25	50	H	2	7	1.35
42	70	210	0.15	2	50	80	H	2	5	1.47
43	75	210	0.45	3	75	50	L	2	3	2.13
44	80	210	0.15	1	25	65	H	3	4	1.18
45	75	200	0.3	3	50	80	D	3	3	1.97
46	75	210	0.15	3	75	80	H	4	6	1.78
47	80	190	0.45	3	75	80	H	2	2	2.06
48	70	190	0.3	1	75	50	L	4	5	2.08
49	80	190	0.45	1	25	80	H	2	2	1.65
50	80	210	0.3	2	25	50	H	4	4	1.87

Table 3: The Statistical Summary Of The Models.

Response	Model	P-value	R2	R2 Adj	Root Mean Squared Error	Precision	Remarks
ΔL	Linear	$5.4 * 10^{-9}$	0.67	0.624	0.0385	Inadequate	
	Interactions	$7.32 * 10^{-9}$	0.887	0.809	0.0275	Inadequate	
	Purequadratic	$6.33 * 10^{-8}$	0.628	0.576	0.0409	Inadequate	
	Quadratic	$4.34 * 10^{-10}$	0.976	0.937	0.0157	Adequate	Selected
ΔW	Linear	$5.14 * 10^{-13}$	0.861	0.821	0.0265	Inadequate	
	Interactions	$5.14 * 10^{-13}$	0.861	0.821	0.0265	Inadequate	
	Purequadratic	$3.31 * 10^{-13}$	0.906	0.865	0.023	Inadequate	
	Quadratic	$5.14 * 10^{-11}$	0.984	0.957	0.013	Adequate	Selected
ΔT	Linear	$2.81 * 10^{-7}$	0.729	0.641	0.0628	Inadequate	
	Interactions	$1.36 * 10^{-7}$	0.774	0.684	0.0589	Inadequate	
	Purequadratic	$2.09 * 10^{-10}$	0.883	0.882	0.0442	Inadequate	
	Quadratic	$3.45 * 10^{-10}$	0.955	0.905	0.0323	Adequate	Selected

$$\Delta W = -7.8175 + 00.16006A + 0.0098978B - 2.3057C + 0.12384D + 0.015365E + 0.01839F + 0.52171G - 0.17844H - 0.00012194AB - 0.0058007AC - 7.7802*10^{-5}AE - 0.00080476AG + 0.00089284AH + 0.0067878BC - 4.246*10^{-5}BE - 0.0018614BG - 0.0021619CE + 0.0028997CF - 0.047168CG + 0.083541CH - 0.00035901DE + 0.00028402DF - 0.0041935DG - 2.303*10^{-5}EF - 0.00085333A^2 + 1.8364C^2 - 0.022442D^2 + 2.2585*10^{-5}E^2 - 0.00012892F^2 - 0.016321G^2 + 0.017576H^2 \quad (7)$$

$$\Delta T = -14.046 + 0.36642A - 0.0068654B + 1.7033C - 0.12077D + 0.0022519E + 0.041985F + 0.0078414G - 0.08295H - 0.003443AD - 8.4681*10^{-5}AE - 0.00024119AF + 0.0037604AG + 0.0018528BD + 0.23827CD + 0.0095769CE - 0.0059142CF + 0.098881CH - 0.019251DG - 4.281*10^{-5}EF - 0.00059124EG + 0.00070657FH - 0.0023279A^2 - 3.7194C^2 + 4.2589*10^{-5}E^2 - 0.00016194F^2 - 0.056329G^2 \quad (8)$$

All developed mathematical models are subject to constraints:

$70 \leqslant A \leqslant 80$

$190 \leqslant B \leqslant 210$

$0.15 \leqslant C \leqslant 0.45$

$1 \leqslant D \leqslant 3$

$25 \leqslant E \leqslant 75$

50⩽ F ⩽ 80
1⩽ G ⩽3
2⩽ H ⩽4

4.2 Checking The Adequacy Of The Data With The Developed Models:

The relevance of the developed models was evaluated at a 95 % confidence interval by applying the ANOVA technique, which is used to evaluate the meaning of the developed models. In order to develop realistic models, the significance terms with the highest partial likelihood values were filtered using the upstream elimination method. P-value for the statistic F hypotheses verifies that the corresponding coefficient is equal to zero or not. For example, the p-value of the F statistic for is greater than 0.05, so this term is not significant at the 5% significance level given the other terms of the model.

The validity of developed regression models was also assessed using normal probability curves. Fig 7 (a - c) shows the normal probability curves of the residues for the dimensional error in length, width and thickness, respectively. These values indicate that the residues lie on a straight line and follow a normal distribution, this indicates that the developed models are well adapted to the experimental values and that the errors are normally distributed.

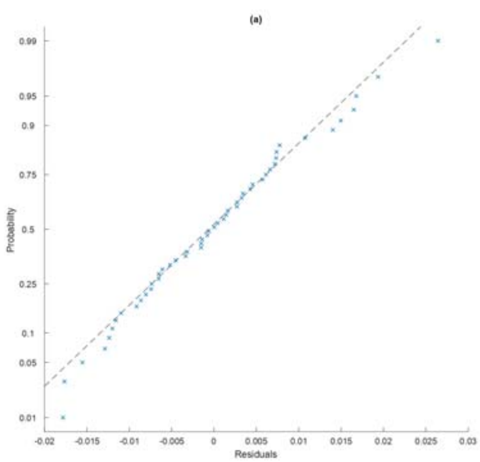

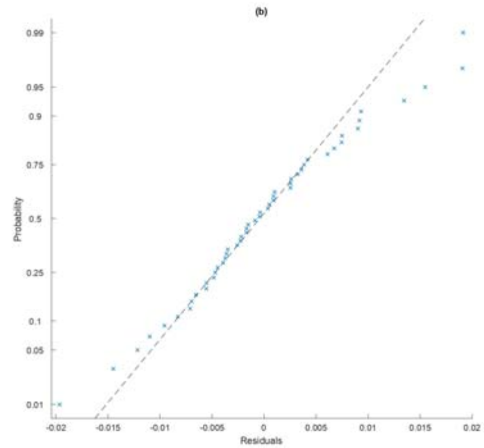

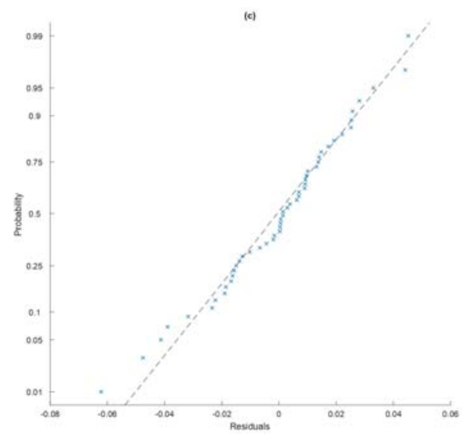

Figure 7: Normal Probability Plot Of Residuals For Variation Of: (A) Length, (B) Width And (C) Thickness

The experimental values were compared to the predicted values of the dimensional error in length, width and thickness calculated from equations 6 to 8. Fig. 8 (a - c) presents predicted values plotted with experimental values for three responses, respectively. It can be noted that there is a high degree of correlation between the predicted values and the experimental values, which implies that the developed models are able to accurately model the relationship between dimensional accuracy and parameters and can produce accurate results.

ISSN: **1992-8645** www.jatit.org E-ISSN: **1817-3195**

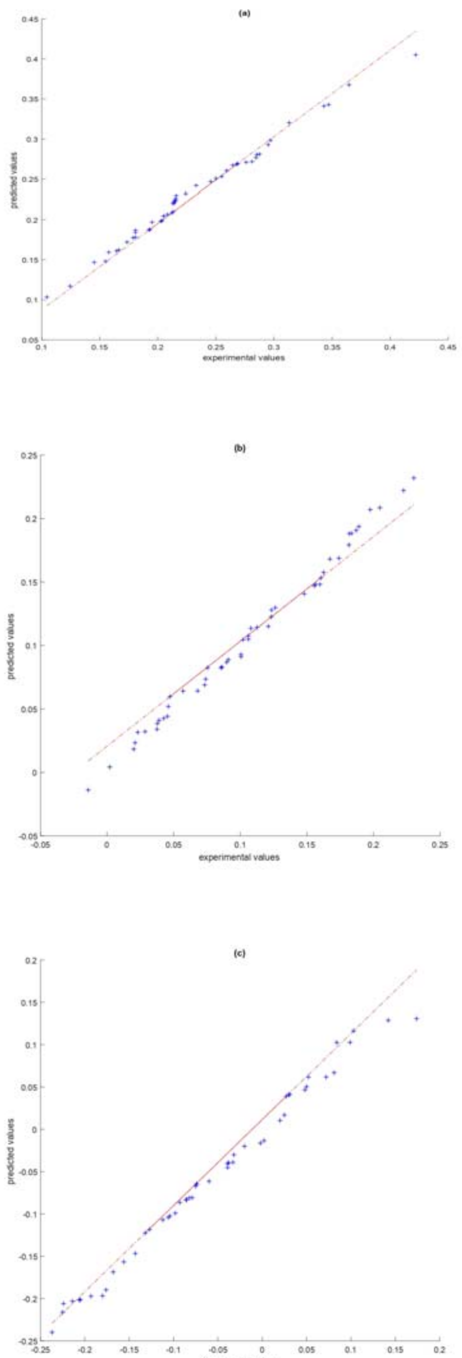

Figure 8: Comparisons Of Experimental Values And Predicted Values For The Variation Of: (A) Length, (B) Width And (C) Thickness

5. RESULTS AND DISCUSSION

In order to verify and understand the effect of the eight process parameters on the three output responses, the 3D response surface curves can be graphically applied to study and analyze the interactions between factors and their main effects on responses, as well as the other factors are held constant at their center value. On the other hand, 3D response surface graphics can be applied to achieve the optimal response of variation in length, width, and thickness. From the developed models, the 3D response surface curves were plotted to understand the behavior of the output responses, which are studied by different levels of process parameters. Figures 9 to 11 show the corresponding 3D response surface plots showing various interactive effects of parameters for the three output responses, respectively comprising the variation in length, width, and thickness. The colored bars in figs.9 to 11 indicate the various effects of the process variables on the response.

5.1 Influence Of Process Parameter On The Dimensional Error Of The Length:

From a global observation of Figure 9 (a - g), a high interaction between deferent process parameters and the change in length was noted. Fig. 9 (a - g) illustrates the 3D surface diagrams between the most significant process parameter interactions for the change in length. In Figure 9 (a) it can be seen that the variation in length between the fabricated part and the dimensional error can be reduced by decreasing the Platform temperature and the thickness of the layer is average value. The variation in length proved to be lower (0.2047 mm) for a the Platform temperature 70 and with a layer thickness of 0.3 mm. Fig 9 (b) illustrates the effect of layer thickness and the extruder temperature on the dimensional error with Platform temperature, Number of shells, Infill density, print speed, Infill pattern and Number of solid layers' U / L are maintained constant to their value in the center. Dimensional imprecision can be caused by the removal of the extruded material as it passes from the semi-molten state to the solid state. Note in Figure 9 (b) that the dimensional error increases when the Extruder temperature is low and the thickness of the layer is at its maximum or minimum value (min is the low value of the thickness of the layer and max value nearest to the diameter of the nozzle). The optimum value of the change in length (0.2254 mm) for this interaction can be obtained with an extruder temperature of 210 and a layer thickness of 0.3 mm. Figure 9 (c) is the graph of the surface response that shows the effect of the

ISSN: 1992-8645 www.jatit.org E-ISSN: 1817-3195

number of contours and the thickness of the layer on the variation of length when other parameters remain constant at their value in the center. As can be seen in this figure, the dimensional error tends to increase steadily as the number of contours increases. The optimum value of the change in length (0.2068 mm) for this interaction can be obtained with a number of contours of 1 and a layer thickness of 0.330 mm. Because lower values of the contours number can reduce deformation by reducing the build-up of heat stress. Figure 9 (d) shows the graph of the response surface of the effect of Infill density and the thickness of the layer on the variation of the length. It has been observed that the dimensional error increases when Infill density increases and the layer thickness at its lowest level. The optimum value of the dimensional error (0.2462 mm) for this interaction can be obtained with an infill density of 25% and a layer thickness of 0.310 mm. The effect of the print speed and the thickness of the layer on the variation of the length have been shown in the graph of the response surface see Figure 9 (e). It has been noticed that the dimensional error increases as the thickness of the weak layer and at any print speed. The optimum value of the dimensional error (0.2553 mm) for this interaction can be obtained with a print speed of 80 mm / s and a layer thickness of 0.330 mm. Infill pattern has a marginal effect on length variation, as shown in Figure 9 (f), but the thickness of the layer has a significant effect on this response. The result states that the dimensional error for this interaction effect can be improved by using the average value of the layer thickness and Infill pattern of the honeycombs. Therefore, the optimal value of the dimensional error (0.2201 mm) for this interaction can be obtained with an infill pattern honeycombs and a layer thickness of 0.3150 mm. Fig. 9 (g) illustrates the effect of the number of solid layers and the thickness of the layer on the dimensional error with the other parameters that have been kept constant at their values in the center. We observe that the dimensional error at its maximum value when the number of solid layers is very large and the thickness of the layer is low. So the optimal value of the dimensional error (0.2575 mm) for this interaction can be obtained with a layer thickness of 0.3250 mm and a number of solid layers of 3.

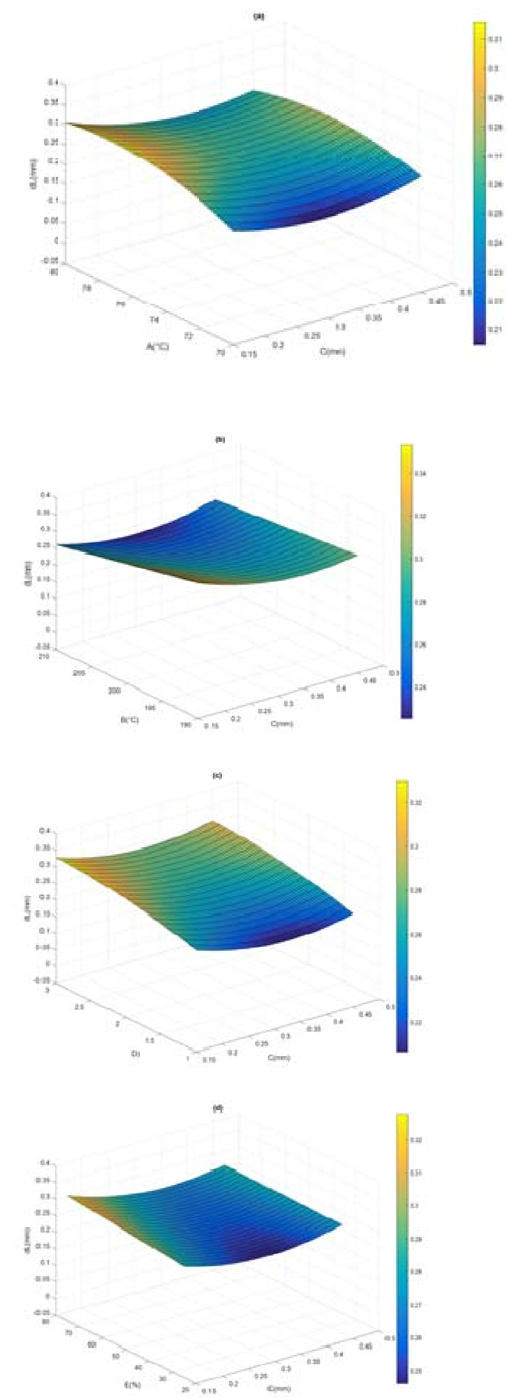

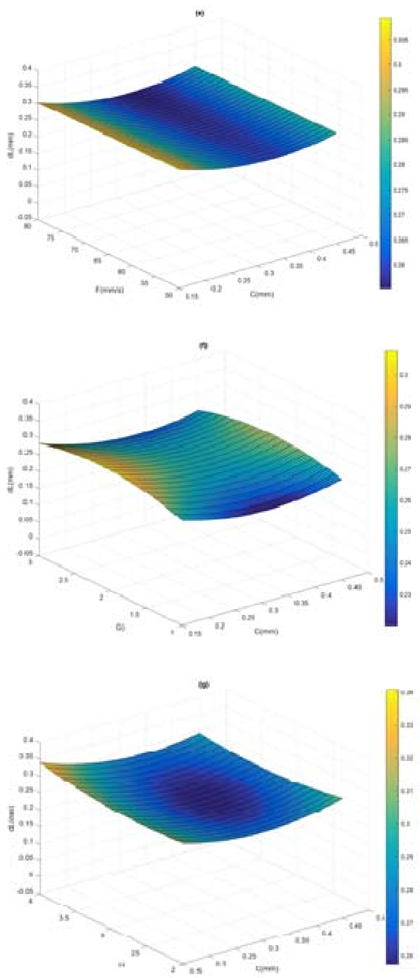

Figure 9: 3D Response Surface Plots Representing Interactive Effects Of Parameters On Change In Length

5.2 Influence Of Process Parameter On The Dimensional Error Of The Width:

Figure 10 (a - g) shows the effect of the most significant interactive terms on the dimensional error of the width by graphs of the response surface. Figure 10 (a) shows the graph of the response surface of the effect of the Platform temperature and the thickness of the layer on the variation of width when other parameters remain constant with their value in the center. Note that the optimal value of the dimensional error of the width (0.0848mm) for this interaction can be obtained with a layer thickness of 0.300 mm and the Platform temperature of 70 . Fig. 10 (b) illustrates the 3D surface graph between the extruder temperature interactions and the thickness of the layer on the change of width. It is noted in Figure 10 (b) that the dimensional error decreases as the Extruder temperature increases. The optimum value of the dimensional error of the width (0.0911 mm) for this interaction can be obtained with a layer thickness of 0.2900 mm and the extruder temperature of 210 . Figure 10 (c) shows the graph of the response surface of the effect of the number of contours and the thickness of the layer on the variation of width when other parameters remain constant at their value in the center. As can be seen in this figure, the dimensional error of the width tends to increase steadily with the increase in the number of contours. The optimal value of the change of width (0.0797mm) for this interaction can be obtained with a number of contours of 1 and a layer thickness of 0.3100mm. Because lower values of the contours number can reduce deformation by reducing the build-up of thermal stress. Figure 10 (d) shows the graph of the response surface of the Infill density effect and the thickness of the layer on the variation of the width. It has been observed that the dimensional error increases when Infill density increases and the thickness of low layer. Therefore, the optimal value of the dimensional error of the width (0.1196 mm) for this interaction can be obtained with an Infill density of 41 % and a layer thickness of 0.3100 mm. The effect of the print speed and the thickness of the layer on the dimensional error of the width have been shown in the graph of the 3D response surface, see Figure 10 (e). It has been noted that the variation in width between the fabricated part and the design dimension (the dimensional error) can be reduced when printing with a low speed and the thickness of the layer is in the average value. The optimum value of the dimensional error (0.0629 mm) for this interaction can be obtained with a layer thickness of 0.3200 mm and a print speed of 50 mm / s. Infill pattern has a marginal effect on the variation of the width, as shown in Figure 10 (f), but the thickness of the layer has a significant effect on this response. Note in Figure 10 (f) that the dimensional error increases when the thickness of the layer is at its maximum or minimum value (min is the low value of the thickness of the layer and maxi the most value close to the diameter of the nozzle) and whatever Infill pattern but it takes the maximum value when using an infill pattern of grid structure with a thickness of the weak layer. Then, the optimal value of the dimensional error (0.1041 mm) for this interaction can be obtained with an infill pattern honeycombs and a layer thickness of 0.3000 mm. Fig. 10 (g) illustrates

ISSN: 1992-8645 www.jatit.org E-ISSN: 1817-3195

the effect of the thickness of the layer and the Number of solid layers on the dimensional error with the other parameters that have been held constant at their center values. We observe that the dimensional error increases when we increase the Number of solid. Therefore the optimal value of the dimensional error (0.1154 mm) for this interaction can be obtained with a layer thickness of 0.3300 mm and a number of solid layers of 2.

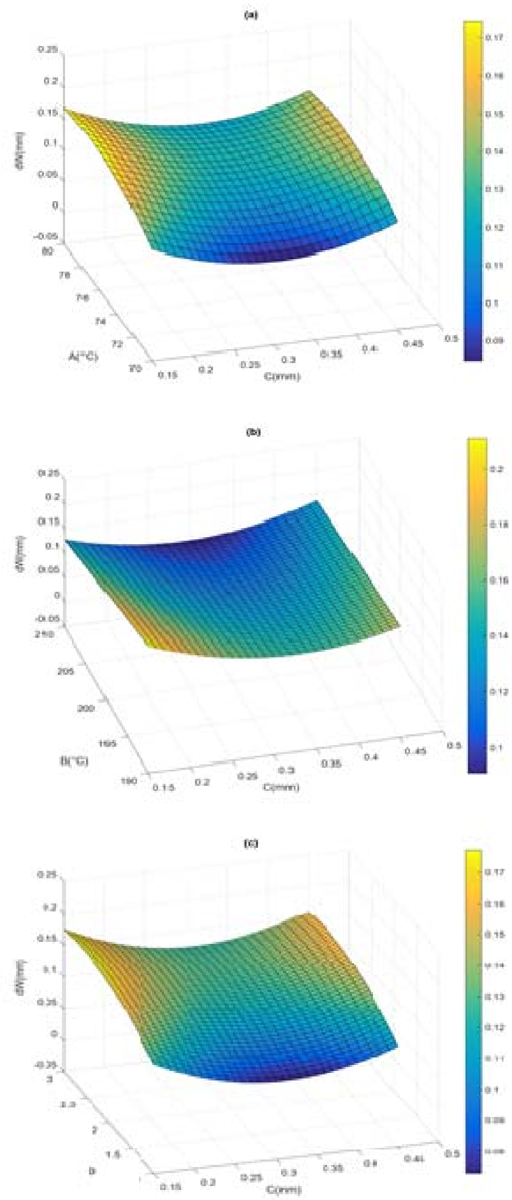

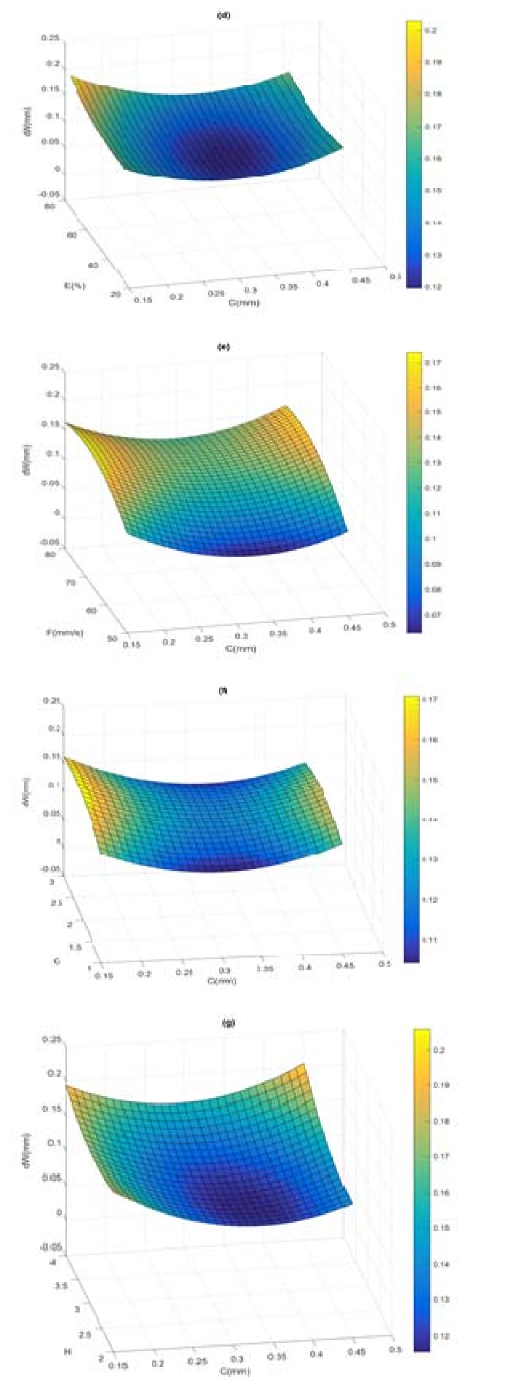

Figure 10: 3D Response Surface Plots Representing Interactive Effects Of Parameters On Change In Width

5.3 Influence of process parameter on the dimensional error of the thickness:

It has been observed experimentally that the thickness of all the printed samples was above or below the nominal value of (3.5mm), which seems to be due to the error of the height of Z. In this experiment, all samples should be printed with a height (H) of 3.5 mm and some samples should have a slicing thickness (C) of 0.1500 mms so the number of layers needed to make these samples is 23.33 layers. However, the sample should be made with a layer thickness of 0.3000 mm, so the number of layers needed is 11.66 layers. Also, for a thickness of 0.4500 mm, it requires 7.77 layers to build the sample. In this case, the machine will deposit 23 layers with a layer thickness of 0.1500 mm, and 12 layers with a layer thickness of 0.3000 mm and 8 layers with a layer thickness of 0.4500 mm. As a result, the actual thickness of the samples manufactured is greater than the designed thickness specified by the CAD model for the thicknesses of the layers equal 0.3000 mm and 0.4500 mm and unlike the thicknesses of the layers is equal 0.1500 mm where the sample is smaller. Therefore, it can be concluded that the difference between the calculated value and the experimental value is important when the layer thickness is large. Figure 11 (a) is the graph of the 3D response area that illustrates the Platform temperature and the thickness of the layer on the variation of the thickness. From this figure, it can be noticed that the dimensional error of the thickness of the part decreases in a linear manner as a function of the decrease of the Platform temperature and the thickness of the layer. The optimum value of variation of the thickness (0.0176mm) for this interaction is obtained at a layer thickness of 0.2100 mm and at a temperature of 70 . The interaction effects between the Extruder temperature and the thickness of the layer on the variation of the thickness are shown in Figure 11 (b). It is clear from this graph of the 3D response surface that the dimensional error increases as the layer thickness increases and the value of the Extrude temperature is low. The optimum value of variation of the thickness (0.0595mm) for this interaction is obtained at a layer thickness of 0.2200 mm and an extruder temperature equal to 205 . Figure 11 (c) is the graph of the surface response that shows the effect of the layer thickness and the number of contours on the dimensional error of the thickness when other parameters remain constant at their center value. As can be seen in this figure, the dimensional error of the thickness tends to increase steadily with the increase in the number of contours and the thickness of the layer. The optimum value of the change in thickness (0.0687mm) for this interaction can be obtained with a number of contours of 3 and a layer thickness of 0.2100 mm. Figure 11 (d) shows the graph of the Infill density effect response surface and the thickness of the layer on the variation of the thickness. It has been noticed that the dimensional error expect the maximum value when the layer thickness is at its average value and low Infill density. Therefore, the optimal value of the dimensional error of the thickness (0.0594mm) for this interaction can be obtained with an Infill density of 75% and a layer thickness of 0.2200 mm. The effect of the print speed and the thickness of the layer on the dimensional error of the thickness have been shown in the graph of the 3D response surface see Figure 11 (e). It has been noticed that the variation of the thickness between the fabricated part and the dimensional error increases when printing with a large print speed and a thickness of the high layer. The optimum value of the dimensional error of the thickness (0.0054mm) for this interaction can be obtained with a layer thickness of 0.2100 mm and a print speed of 50mm / s . Infill pattern has an effect on the variation of the thickness, as shown in Figure 11 (f) , but the thickness of the layer has a significant effect on this response. We note in Figure 11 (f) that the dimensional error wait for the maximum value when the layer thickness and Infill pattern at its mean values. Then, the optimal value of the dimensional error (0.0127mm) for this interaction can be obtained with an infill pattern honeycombs and a layer thickness of 0.2200 mm . Fig. 11 (g) illustrates the effect of the layer thickness and the Number of solid layers on the dimensional error of the thickness with the other parameters that have been kept constant at their center values. It is observed that the dimensional error increases when increasing the thickness of the layer. Therefore the optimal value of the dimensional error (0.0692mm) for this interaction can be obtained with a layer thickness of 0.2200 mm and Number of solid layers of 3.

ISSN: 1992-8645 www.jatit.org E-ISSN: 1817-3195

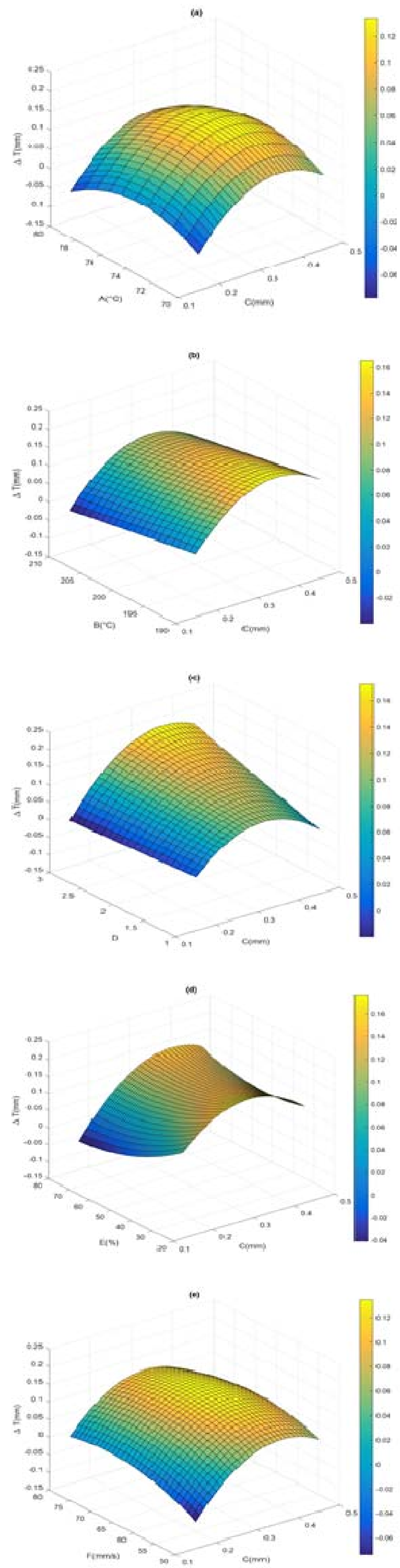

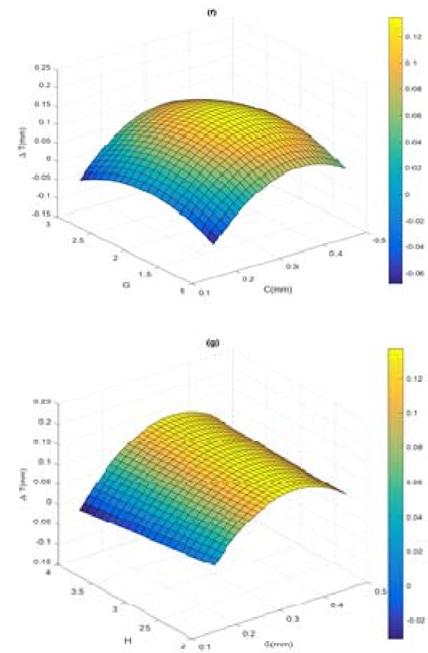

Figure 11: 3D Response Surface Plots Representing Interactive Effects Of Parameters On Change In Thickness

6. CONCLUSIONS

This study represented a methodology for an efficient optimization of FDM technology parameters using D-optimal design. The study showed a successful application of D-Optimal design in optimizing FDM process parameters. The presented method can solve the quality problems (dimensional accuracy) of FDM parts containing a large number of parameters and levels that cannot be chosen by the traditional experimental design when multiple restrictions and physical constraints applied to the experimental variables are included.

In this paper, mathematical representations have been developed to model the relationship between dimensional accuracy and input parameters. The following conclusions are drawn from the results obtained by this study.

- ✓ The results of the statistical analysis have shown that developed regression representations can model the relationship between dimensional accuracy and input parameters with a 95% sureness interval.
- ✓ Parameters (Platform temperature (A); Extrude temperature (B); Layer thickness (C); Number of shells (D); Infill density (E); Print speed (F); Infill pattern (G); solid layers

U / L (H)) show a significant effect on the variation of the length. Thereafter, 3D response surface graph s optimal values are 70 (A), 210 (B), 0.3mm (C), 1 (D), 25% (E), 50mm / s (F)), Infill pattern honeycombs and 3 (H).

- ✓ Optimal values for variation of the width from the 3D response surface graphs are a Platform temperature of 70 , an Extruder temperature of 210 , a Layer thickness of 0.3000mm, a Number of shells of 1 , Infill density of 25%, a Print speed of 50mm / s , Honeycombs infill pattern and 3 solid layers 'U / L'.
- ✓ Optimal values for the variation of the height from the 3D response surface graphs are a Platform temperature of 70 , an Extruder temperature of 205 , a Layer thickness of 0.2200mm, Number of shells of 3 , Infill density of 75%, a Print speed of 50mm / s, Infill pattern honeycombs and 3 solid layers 'U / L'.

All the results presented in this study confirmed that the proposed method was an effective and adequate technique for optimizing FDM process parameters. This method can be applied to guide the new uses of computer optimized design in optimizing FDM process parameters for part quality in other additive manufacturing processes involving a wide range of pro parameters.

REFERENCES

[1] A. Gebhardt, Rapid Prototyping–Rapid Tooling–Rapid Manufacturing, Carl Hanser, Munchen, 2007.

[2] I. Gibson, D. W. Rosen, B. Stucker, et al., Additive manufacturing technologies, Vol. 17, Springer, 2014 (2014)

[3] R. Hague, S. Mansour, N. Saleh, Material and design considerations for rapid manufacturing, International Journal of Production Research 42 (22) (2004) 4691–4708 (2004).

[4] U. Berger, A. Hartmann, D. Schmid, Additive Fertigungsverfahren: Rapid Prototyping, Rapid Tooling, Rapid Manufacturing, Europa-Lehrmittel, 2013 (2013).

[5] T. Lieneke, V. Denzer, G. A. Adam, D. Zimmer, Dimensional tolerances for additive manufacturing: Experimental investigation for fused deposition modeling, Procedia CIRP 43 (2016) 286–291 (2016).

[6] T. Wohlers, Wohlers report 2013: Additive manufacturing state of the industry annual worldwide progress report, wohlers associates, Inc., Colorado, USA (2013).

[7] A. Gebhardt, J. Kessler, L. Thurn, 3D-Drucken: Grundlagen und Anwendungen des additive manufacturing (AM), Carl Hanser Verlag GmbH Co KG, 2016 (2016).

[8] M. Gebler, A. J. S. Uiterkamp, C. Visser, A global sustainability perspective on 3d printing technologies, Energy Policy 74 (2014) 158–167 (2014).

[9] B. Kianian, Wohlers report 2017: 3d printing and additive manufacturing state of the industry, annual worldwide progress report: Chapters titles: The Middle East, and other countries (2017).

[10] T. Srivatsan, T. Sudarshan, Additive manufacturing: innovations, advances, and applications, CRC Press, 2015 (2015).

[11] H. N. Chia, B. M. Wu, Recent advances in 3d printing of biomaterials, Journal of biological engineering 9 (1) (2015) 4 (2015).

[12] F. P. Melchels, J. Feijen, D. W. Grijpma, A review on stereolithography and its applications in biomedical engineering, Biomaterials 31 (24) (2010) 6121–6130 (2010).

[13] I. Gibson, D. Shi, Material properties and fabrication parameters in selective laser sintering process, Rapid prototyping journal 3 (4) (1997) 129–136 (1997).

[14] J. W. Stansbury, M. J. Idacavage, 3d printing with polymers: Challenges among expanding options and opportunities, Dental Materials 32 (1) (2016) 54–64 (2016).

[15] J.-P. Kruth, X. Wang, T. Laoui, L. Froyen, Lasers and materials in selective laser sintering, Assembly Automation 23 (4) (2003) 357–371 (2003).

[16] B. N. Turner, S. A. Gold, A review of melt extrusion additive manufacturing processes: Ii. Materials, dimensional accuracy, and surface roughness, Rapid Prototyping Journal 21 (3) (2015) 250–261 (2015).

[17] N. Guo, M. C. Leu, Additive manufacturing: technology, applications and research needs, Frontiers of Mechanical Engineering 8 (3) (2013) 215–243 (2013).

[18] W. E. Frazier, Metal additive manufacturing: a review, Journal of Materials Engineering and Performance 23 (6) (2014) 1917–1928 (2014).

ISSN: 1992-8645 www.jatit.org E-ISSN: 1817-3195

[19] O. A. Mohamed, S. H. Masood, J. L. Bhowmik, Optimization of fused deposition modeling process parameters: a review of current research and future prospects, Advances in Manufacturing 3 (1) (2015) 42–53 (2015).

[20] C. Vasques, R. Moreira, J. D. Rodrigues, Viscoelastic damping technologies-part ii: Experimental identification procedure and validation., Journal of Advanced Research in Mechanical Engineering 1 (2) (2010).

[21] H. Lu, Y. Obeng, K. Richardson, Applicability of dynamic mechanical analysis for cmp polyurethane pad studies, Materials Characterization 49 (2) (2002) 177–186 (2002).

[22] I. ASTM, Astm52921-13 standard terminology for additive manufacturing coordinate systems and test methodologies, West Conshohocken: ASTM International (2013).

[23] O. A. Mohamed, S. H. Masood, J. L. Bhowmik, Optimization of fused deposition modeling process parameters for dimensional accuracy using i-optimality criterion, Measurement 81 (2016) 174–196 (2016).

[24] S. Masood, K. Alamara, J. Hasan, Developments in scaffold design and manufacturing in tissue engineering (2009).

[25] K. Thrimurthulu, P. M. Pandey, N. V. Reddy, Optimum part deposition orientation in fused deposition modeling, International Journal of Machine Tools and Manufacture 44 (6) (2004) 585–594 (2004).

[26] G. C. Onwubolu, F. Rayegani, Characterization and optimization of mechanical properties of abs parts manufactured by the fused deposition modelling process, International Journal of Manufacturing Engineering 2014 (2014).

[27] S. K. Panda, S. Padhee, S. Anoop Kumar, S. S. Mahapatra, Optimization of fused deposition modelling (fdm) process parameters using bacterial foraging technique, Intelligent information management 1 (02) (2009) 89 (2009).

[28] V. N. Patel, M. K. P. Kadia, V. N. Patel, M. K. P. Kadia, Parametric optimization of the process of fused deposition modeling in rapid prototyping technology-a review, Int. J. Innov. Res. Sci. Technol 1 (7) (2014) 80–82 (2014).

[29] A. Qattawi, B. Alrawi, A. Guzman, et al., Experimental optimization of fused deposition modelling processing parameters: a design for-manufacturing approach, Procedia Manufacturing 10 (2017) 791-803 (2017).

[30] T. Nancharaiah, D. R. Raju, V. R. Raju, An experimental investigation on surface quality and dimensional accuracy of fdm components, International Journal on Emerging Technologies 1 (2) (2010) 106-111 (2010).

[31] R. K. Sahu, S. Mahapatra, A. K. Sood, A study on dimensional accuracy of fused deposition modeling (fdm) processed parts using fuzzy logic, Journal for Manufacturing Science & Production 13 (3) (2013) 183-197 (2013).

[32] T. Lieneke, V. Denzer, G. A. Adam, D. Zimmer, Dimensional tolerances for additive manufacturing: Experimental investigation for fused deposition modeling, Procedia CIRP 43 (2016) 286-291 (2016).

[33] A. K. Sood, R. Ohdar, S. S. Mahapatra, Improving dimensional accuracy of fused deposition modelling processed part using grey taguchi method, Materials & Design 30 (10) (2009) 4243-4252 (2009).

[34] V. B. Nidagundi, R. Keshavamurthy, C. Prakash, Studies on parametric optimization for fused deposition modelling process, Materials Today: Proceedings 2 (4-5) (2015) 1691-1699 (2015).

[35] J. W. Zhang, A. H. Peng, Process-parameter optimization for fused deposition modeling based on taguchi method, in: Advanced Materials Research, Vol. 538, Trans Tech Publ, 2012, pp. 444-447 (2012).